Supporting Information

Schmid et al. 10.1073/pnas.1218311110

SI Experimental Procedures

Zebrafish. Zebrafish embryos were kept at 28.5 °C and were staged according to ref. 1. The wild-type line AB was used for all experiments unless stated otherwise. All experiments were performed in accordance with animal protection standards of the Ludwig-Maximilians University Munich and were approved by the government of Upper Bavaria (Regierung von Oberbayern, Munich, Germany).

ZFN and Identification of Induced Genomic Lesions. CompoZr Custom zinc finger nucleases (ZFN) (Sigma) were designed for the *tardbp* and the *tardbpl* locus. ZF nucleotide recognition sequences are highlighted in uppercase and boldface:

tardbp ZFN set 1:
24342 caGGCAGCCGAAGCAACATGGGT**GGTGGTGGTGGGGGT**ag
24341 gt**CCGTCGGCTTCGTTG**TACCCACCACCACCACCCCCAtc
tardbp ZFN set 2:
24318 gcTTCCGGAGCCCAGTGTCTCAGTG**CATGAGGGGGGGTTCG**tc
24317 cg**AAGGCCTCG**g**GTCACA**GAGTCACGTACTCCCCCCAAGCag
tardbp ZFNset 3:
24320 tcCGGAGCcCAGTGTCTCAGTGCAT**GAGGGGGGT**t**CGTCTG**gt
24319 ag**GCCTCG**g**GTCACAGAG**TCACGTACTCCCCCCAAGCAGACca
tardbpl ZFN set 1:
24350 acCGAAGCCCCGTGTCCCAGTGCA**TGAGAGGGGTCCGAC**ta
24351 tg**GCTTCGGGG**ca**CAGGGT**CACGTACTCTCCCCAGGCTGat
tardbpl ZFN set 3:
24356 acCGAAGCCCCGTGTCCCAGTGCATGA**GAGGGGTCCGACTAG**tg
24353 tg**GCTTCG**g**GGCACAGGGTCA**CGTACTCTCCCCAGGCTGATCac
tardbpl ZFN set 4:
24360 ccCGTGTCCCAGTGCATGAGAGGGG**TCCGAC**t**AGTGGAGGG**gg
24359 gg**GCACAG**g**GTCACGTAC**TCTCCCCAGGCTGATCACCTCCCcc

Genomic lesions induced by ZFN were identified by PCR amplification around the ZFN cut site and restriction fragment length polymorphism analysis. The efficiency of the different ZFN sets to introduce germ-line mutations varied from 5–60%.

PCR amplification of genomic DNA was performed with the following primers:

tardbp exon2 forward: GAGTGCTGTGAATTTAAACATTT
tardbp exon2 reverse: GCAATTGTGCATGTTTTCAGG
tardbp exon6 forward: GAAGAAATTTCCAACTTCTTTC
tardbp exon6 reverse: ACTTACCAAAACACGCTAGG
tardbpl exon1 forward: ATGACGGAGTGCTATATTCG
tardbpl exon1 reverse: *caggaaacagctatgacc*GGATAATTAACCACGTACACCAGATTGCCCCAGTCTGCTTCTGGTGCA**g**gaagaacc (**g** represents mutated Hin1II site; M13 site for sequencing in italics)

Eight microliters of the 18-μL PCR reactions were subsequently digested at 37 °C for 3 h with the respective enzymes:

tardbp exon2 PCR: Alw26I (Fermentas)
tardbp exon6 PCR: CspCI (New England Biolabs)
tardbpl exon1 PCR: Hin1II (Fermentas)

Immunohistochemistry. Embryos were fixed in 4% (wt/vol) paraformaldehyde (PFA) overnight at 4 °C. Embryos were washed twice 10 min in PBST (PBS with 0.1% Tween 20) and dehydrated 10 min in 25%, 50%, 75%, 100%, and 100% (vol/vol) methanol, respectively. The embryos were further incubated in 100% methanol overnight at −20 °C. Subsequent rehydration was done for 10 min in 75%, 50%, and 25% methanol, respectively, followed by one short PBST and two 10-min PBST washes. Embryos at 1.5 days postfertilization (dpf) were additionally incubated for 10 min in 10 μg/mL Proteinase K. Embryos stained with znp-1 antibody at 1 dpf were treated for 6.5 min with 1 mg/mL Collagenase. Embryos were then washed twice for 10 min with PBST and rinsed twice with PBST. Embryos were preincubated for 1 h in newborn calf serum with 0.1% (vol/vol) Tween 20 (NCST) and then incubated overnight in the respective primary antibody in NCST at 4 °C followed by two short PBST washes and four washes for 30 min in PBST. Preincubation with NCST for 1 h was followed by secondary antibody incubation overnight at 4 °C in NCST. The embryos were washed for 30 min twice with PBST and 4 × 5 min with PBST. Nuclear DAPI counterstain was done with 5 ng/μL DAPI (Roche) incubated for 1 h and then washed twice with PBST.

Whole-Mount in Situ Hybridization. Specific in situ probes were generated targeting the 3′UTR of *tardbp* and *tardbpl*.

The *tardbp* 3′ UTR was amplified from EST clone 3819280 (IMAGE ID) using the following primers:

tardbp UTR forward: GCTTTGTGTTTGAAGTGTCG
tardbp UTR reverse: AAGCACTCCCTTCATTTGAC

The *tardbpl* 3′ UTR was amplified from EST clone 2640053 (IMAGE ID) using the following primers:

tardbpl UTR forward: TCAAAGAGCACAGCTTCACT
tardbpl UTR reverse: AATATCCTGCCAGTGACTCA

The respective PCR products were cloned in pCRII-TOPO (Invitrogen), sequenced, linearized using BamHI and XhoI, and in vitro transcribed using T7 or SP6 Polymerase (Fermentas) and DIG RNA labeling mix (Roche). Next, 1 ng/μL RNA was used for in situ hybridization.

In situ probes *cardiac myocyte light chain 2* (*cmlc2*) and *atrial myosin heavy chain* (*amhc*) were previously described (2). For whole-mount in situ hybridization embryos were fixed in 4% PFA overnight at 4 °C. Embryos were washed twice for 10 min in PBST and with 100% methanol for 15 min. The embryos were incubated in 100% methanol overnight at −20 °C. Rehydration through a 75%, 50%, 20% methanol series for 5 min and each was followed by 3 × 5 min washes with PBST. The 1.5- and 2-dpf-old embryos were additionally treated with Proteinase K (10 μg/mL in PBST) for 30 min and washed 5 min with PBST. After refixing with 4% PFA for 20 min at room temperature they were washed twice for 5 min with PBST. Embryos were transferred in 500 μlL HYB^+ [50% (vol/vol) formamide, 5× SSC, 0.1% Tween 20,

5 mg/mL torula RNA, 50 μg/mL heparin] and prehybridized at 65 °C for 3 h. Antisense RNA probe (50-ng probe in 100 μL HYB^+) was added and incubated at 65 °C overnight. After probe removal embryos were washed twice 45 min with 50% formamide/2× SSCT, 1× 15 min 2× SSCT, 2× 45 min 0.2× SSCT. All washes were performed at 65 °C. After 3-h incubation in NCST at room temperature the Fab-AP antibody in NCST (1:4,000 dilution) was added and incubated overnight at 4 °C. Antibody was washed off 4 × for 25 min with NCST. Embryos were washed 3 × 5 min with staining buffer NTMT (100 mM Tris pH 9.5, 50 mM $MgCl_2$, 100 mM NaCl, 0.1% Tween 20) and subsequently stained with NTMT with 0.25 mg/mL Levamisol (AppliChem) and 4.5 μL NBT and 3.5 μL X-Phosphate (BCIP) per milliliter NTMT.

Cloning. For all cDNA cloning purposes, 2 dpf AB cDNA was used as a template. The following primers were used:

tardbpl forward: ATGACGGAGTGCTATATTCG
tardbpl-V5 reverse: TCACGTAGAATCGAGACCGAGGAGAGGGTTAGGGATAGGCTTACCTCCTCCTCCTCCTCCCACATGGGAAGAAGGGAAC
tardbpl_tv1 forward: ATGACGGAGTGCTATATTCG
tardbpl_tv1-V5 reverse: TCACGTAGAATCGAGACCGAGGAGAGGGTTAGGGATAGGCTTACCTCCTCCTCCTCCTCCCATTCCCCAACTGGACTTTGTC

FUS was amplified from a template, pcDNA3.1 FUS, previously described in ref. 3:

FUS forward:
CCGCTCGAGGCGGACATGTACCCATACGACGTCCCAGACTACGCTGCCTCAAACGATTATACCCAA
FUS reverse:
CGGGATCCTTAATACGGCCTCTCCCTGCGATCCTGTCTG

All PCR products were cloned in the pCR8/GW/TOPO vector (pCR8/GW/TOPO/TA cloning kit; Invitrogen) and further recombined with LR Clonase II (Invitrogen) in $pCS2^+$/GW-A (generated with the Gateway Conversion System; Invitrogen) to in vitro synthesize mRNA. TDP-43 constructs were previously described in ref. 4.

Knockdown. Knockdown of Tardbp was done by microinjection of an antisense gripNA (Active motif) targeting the translation initiation site of *tardbp*. The Tardbp protein levels were reduced by 95% compared with wild-type levels (Fig. S3*A*) upon microinjection of 2–4 pL of 1 mM *tardbp* ATG-2 grip. The following grip was used: *tardbp* ATG-2 ACATCTCGGC**CAT**CTTTC (start codon in boldface).

mRNA Injections. mRNA was synthesized in vitro using the mMessage mMACHINE kit (Ambion) according to the manufacturer's instructions. ZFN mRNA was injected at a concentration of 400 ng/μL. *TDP-43*;*TDP-43*^{G384C}, *tardbp*, and *tardbpl* mRNAs were carefully titrated to avoid toxicity and injected at a concentration of 150 ng/μL. *FUS* mRNA was injected at a concentration up to 700 ng/μL to assure high protein expression. Successful translation of injected mRNAs was controlled by Western blot analysis.

RT-PCR. Total RNA isolation from embryos was performed with the RNeasy kit (Qiagen) according to the manufacturer's instructions with on column DNase I (Qiagen) digestion. The first strand cDNA synthesis was performed with the M-MLV reverse transcriptase (Invitrogen) and random hexamer primers (Fermentas) according to the manufacturer's instructions.

Primers used for detection of *tardbpl_tv1* by RT-PCR:

Primer pair 1:
tardbpl RT for: CTGCGGCCTAAGATACCGA
tardbpl_tv1 RT rev: GGCAAATATTTAAGGGAAATAATA
Primer pair 2:
tardbpl start for: ATGACGGAGTGCTATATTCG
tardbpl_tv1 RT rev: TCAAATCTCTCCCTACATTCC
actin for: TGTTTTCCCCTCCATTGTTGG
actin rev: TTCTCCTTGATGTCACGGAC

Quantitative RT-PCR. Human brain material for expression analysis was provided by the Flanders-Belgian Biobank of the Neurodegenerative Brain Diseases group of the Vlaams Instituut voor Biotechnologie department of molecular genetics, Antwerp, Belgium. The biobank systematically collects human biomaterials (DNA, serum, plasma, fibroblasts, cerebrospinal fluid, EBV-transformed lymphoblasts, frozen and formalin-fixed brain) together with medical and demographic information of dementia patients for translational genetic studies.

For the present study, total RNA was provided from autopsied brains (frontal cortex) of 13 patients [11 frontotemporal lobar degeneration (FTLD) and 2 Alzheimer's disease cerebral amyloid angiopathy (AD-CAA)] and 12 control individuals. The patient group consisted of five patients with FTLD-TDP (Tar DNA binding protein) histopathology proven $TDP\text{-}43^+$ brain pathology with unidentified genetic cause [average age at onset: 66 (range 47–80) years, average age at death 72 (range 50–88 y)] (5). Another six patients had FTLD-TDP brain pathology as a result of a GRN mutation, average age at onset: 66 (range 57–70) y, average age at death 69 (range 62–75 y) (6). Two patients died of Alzheimer's disease (age at onset available for one patient: 61 y, age at death 74 y) and showed Alzheimer's disease neuropathology with a strong CAA component. Average age at death in the control individuals who did not show neuropathology was 74 (62–87) y.

For RNA extraction, 30–50 mg of fresh-frozen frontal cortex was ground in liquid nitrogen. Total RNA extraction was performed using the Ribopure kit (Ambion, Applied Biosystems) and treated with DNase (Turbo DNase Kit; Ambion, Applied Biosystems). The integrity and quality of all human RNAs was verified by Agilent Bioanalyzer analysis to measure RNA integrity. RNA integrity values varied from 5.3 to 8.4. cDNA synthesis was carried out using the Taqman MicroRNA Reverse Transcription Kit (Applied Biosystems) following the manufacturer's instructions using random hexamer primers (Sigma Aldrich). Quantitative Real Time PCR of human *Filamin C* (*hFLNC*) was performed using SsoFast Evagreen Supermix (BioRad) with standard protocols.

The following primers were used:

hFLNC sense short: GCAGCCGGTGAGGGGAAGGT
hFLNC antisense short: CTCCTCTGTGGCCAGCACGT
hFLNC sense long: TGGATGCCAAGGCAGCCGGT
hFLNC antisense long: CTCCTCCTCGTGCGGCAG
All samples were run in triplicates and normalized to the endogenous housekeeping genes amplified with the following primers:
GAPDH sense: CTGCACCACCAACTGCTTAG
GAPDH antisense: GTCTTCTGGGTGGCAGTGAT
YWHAZ sense: TGAGCAGAAGACGGAAGGTGCTG
YWHAZ antisense: TCTGATGGGGTGTGTCGGCTGC

Relative mRNA abundance was calculated using the $\Delta\Delta C_t$ method. Statistical analyses were performed with Mann–Whitney testing using the GraphPad Prism 5 Software.

Ethical Insurance. The genetic, clinical, and pathological study of FTLD patients and control individuals was approved by the Ethical committees of the University of Antwerp, The Antwerp University Hospital, and the Hospital Network Antwerp Middelheim Hospital. All participants signed informed consent forms

for clinical and genetic research and their data and samples were stored in the LIMS database using unique identifiers to protect the participants' privacy.

Antibodies.

TDP-43 (Sigma SAB420006), WB 1:10,000
TDP-43 (Novus Biologicals NB110-55376), WB 1:2,000
TDP-43 (Cosmo Bio CAC-TIP-TD-P09), WB 1:8,000
Vinculin (Sigma-Aldrich V4505), IF 1:50
α-Actinin (Sigma-Aldrich A7811), IF 1:500
znp-1 (DSHB), IF 1:100
acetylated Tubulin (Sigma T6793), IF 1:100
ZE-BO-1F4, (rat IgG2a), IF 1:1 (7)
α-Tubulin (Sigma T6199), WB 1:8,000
Anti-mouse IgG, HRP conj. (Promega, W4021), WB 1:5,000
Anti-rabbit IgG, HRP conj. (Promega, W4011), WB 1:10,000
Alexa Fluor antibodies (Invitrogen), IF 1:500

The following antibodies were generated by the Institute of Molecular Immunology, Helmholtz Center Munich by standard procedures:

Tardbpl 8G1 (Tardbpl epitope: KYFLEQAGPD), WB 1:1, rat IgG2c
Tardbpl_tv1 16C8-11 (Tardbpl_tv1 epitope: SRQMMDRGRFGGYG), WB 1:10, rat IgG2a
Tardbpl 5F5-11 (Tardbpl epitope: FERSQYQFPSSHV), WB 1:1, rat IgG2a
Tardbp 4A12-111 (Tardbp epitope: TSTSGTSSSRDQAQTY), WB 1:1, rat IgG2a
Anti-rat IgG2c, HRP conj., WB 1:16,000
Anti-rat IgG2a, HRP conj., WB 1:12,000

Western Blotting. Embryos were frozen in liquid nitrogen and lysed in 4× Lämmli buffer by sonication. Lysates were boiled for 5 min at 95 °C while shaking at 800 rpm. Supernatant was loaded after a 5-min spin at 13,000 rpm at room temperature. A total of 0.5–1.0 embryos per lane and about one-tenth of an adult brain per lane were loaded on 12% (wt/vol) Tris glycine gels. After electrophoresis, probes were transferred to PVDF membranes (Millipore). Membranes were blocked for 1 h in TBST with 3% fat free milk powder. The primary antibody was incubated in block solution overnight at 4 °C. After washing 4 × 15 min with TBST with 3% fat-free milk powder, the secondary antibody was incubated for 1 h in TBST with 3% (wt/vol) fat-free milk powder. Development of the membrane after 6 × 15 min TBST washes was performed with ECLplus (Amersham).

Microangiography. Microangiography was performed as previously described (8).

Electron Microscopy. Zebrafish embryos at 2 dpf were cut in half crosswise and the posterior half was high-pressure frozen immediately in a Bal-Tec HPM 010. Freeze substitution was carried out in a Leica AFS2 at −90 °C for 100 h in 0.1% (vol/vol) tannic acid, 7 h in 2% (vol/vol) OsO_4, and at −20 °C for 16 h in 2% OsO_4, followed by embedding in EPON at room temperature. Next, 50-nm cross-sections were poststained with saturated uranyl acetate in 75% methanol and 4% (wt/vol) lead citrate (9). Micrographs were taken with a 1,024 × 1,024 CCD detector (Proscan CCD HSS 512/1024; Proscan Electronic Systems) in a Zeiss electron microscop 902A, operated in the bright-field mode.

Proteomics. Sample preparation for mass spectrometry was performed as previously described (10). In brief, pools of 16 1.5-dpf-old deyolked embryos were lysed in 300 μL lysis buffer [4% (wt/vol) SDS, 100 mM Tris pH 7.6, 100 mM DTT] at 95 °C and consecutively sonicated for 30 s (Cell Disruptor B15; Branson). Samples were centrifuged at 10,000 × *g* to remove insoluble cellular debris. Upon addition of an equal volume of 8 M urea, one-third of the cell lysate was added to a 30-kDa vivacon spin column (Sartorius Stedim). Filter-aided sample preparation was performed as previously described (11). To allow quantitative comparison between the samples obtained from wild-type and *tardbp*$^{-/-}$;*tardbpl*$^{-/-}$ double-knockout fish, dimethyl-labeling was applied as previously described (12). Peptides resulting from the tryptic digest of the wild-type fish were labeled "light" using undeuterated formaldehyde (Fluka), and peptides from the double-knockout fish were labeled "heavy" using deuterated formaldehyde (Aldrich). Labeled peptides from both conditions were mixed in a 1:1 ratio and dried in a speed-vacuum centrifuge. To reduce the complexity of peptide mixture, stage tip-based anion exchange chromatography was applied (13). Five fractions were obtained using elution buffers with a pH of 11, 8, 6, 5, and 3. Every fraction was analyzed twice in a LC-MS/MS set-up consisting of an Easy nLC II (Proxeon) and an LTQ-Velos Orbitrap mass spectrometer (ThermoFisher Scientific). Samples were separated on 15-cm capillary emitter columns (New Objective; FS360-75-8-N-S-C15) packed in-house with 2.4-μm C18 material (ReproSil-Pur 120 C18-AQ; Dr. Maisch GmbH) applying 200-min gradients ranging from 7–42% (vol/vol) acetonitrile. The gradient consisted of two linear sections (7–25% acetonitrile in the first 167 min and 25–42% acetonitrile in the following 36 min). Full FTMS scans were obtained at a resolution of 60,000 with 1,000,000 as FTMS full AGC target and recorded in profile mode. Up to the 14 most-intense ions from each full FTMS scan were isolated and fragmented by collision-induced dissociation fragmentation with an isolation width of 2 Da and enabled wideband activation. Selection of the top 14 precursor ions was restricted by a dynamic exclusion list (50-s exclusion time, 500 ion list size) and charge-state screening with enabled monoisotopic precursor selection. MS2 spectra were recorded in centroid mode in the linear ion trap with 10,000 as ion trap AGC target value. Data analyses were performed using the freely available MaxQuant software suite (v1.2.0.11) with the embedded Andromeda search algorithm for protein identification (14, 15). Most default settings of the software suite including a false-discovery rate of less than 1% at peptide and protein level were applied (exceptions: modifications were set according to the dimethyl-labeling protocol, three missed cleavages were allowed and a second peptide search was performed). Database search was performed using the *Danio rerio* IPI database (v3.86). As filter criteria for the final dataset, at least two unique peptides per protein group were required as well as a possible quantification of the respective protein group in at least two of the three biological replicates. From the two technical replicates of each biological replicate, the mean ratio was calculated on the basis of the normalized heavy/light (H/L) isotope ratios (equates the ratio of protein level of the respective protein group between the double knock out and the wild-type fish). For final quantification of the protein levels, the mean from the three biological replicates was determined as well as the SEM as a measurement for the variability between the replicates. A *P* value was calculated for every protein on the basis of a Student *t* test. The abundance ratios from the different biological replicates of the respective protein were compared with the mean abundance ratios of the reference proteins in the different biological replicates. A *P* value below 0.05, an increase or decrease of protein abundance by at least 30% and the quantification of the respective protein in at least two biological replicates were defined as the inclusion criteria for the final hit list. For better graphic display of single peptide spectra, raw data were also analyzed using the Proteome Discoverer Suite 1.2 (ThermoFisher Scientific) with the embedded SEQUEST algorithm for protein identification as described previously (16).

Image Acquisition. Images were taken with an Axioplan2 compound microscope (Zeiss) and a Cell observer spinning-disk microscope (Zeiss). Brightness and contrast were adjusted using Axiovision (Zeiss) and Fiji.

Movie Acquisition. Movies S1, S2, S3, and S4 were taken with a Cell observer spinning-disk microscope (Zeiss). Movie S5 was recorded with a digital video camera DCR-PC101E (Sony) mounted on a Stemi stereomicroscope (Zeiss).

1. Kimmel CB, Ballard WW, Kimmel SR, Ullmann B, Schilling TF (1995) Stages of embryonic development of the zebrafish. *Dev Dyn* 203(3):253–310.
2. Langenbacher AD, et al. (2011) The PAF1 complex differentially regulates cardiomyocyte specification. *Dev Biol* 353(1):19–28.
3. Dormann D, et al. (2010) ALS-associated fused in sarcoma (FUS) mutations disrupt Transportin-mediated nuclear import. *EMBO J* 29(16):2841–2857.
4. Dormann D, et al. (2009) Proteolytic processing of TAR DNA binding protein-43 by caspases produces C-terminal fragments with disease defining properties independent of progranulin. *J Neurochem* 110(3):1082–1094.
5. Langenhove Van T, et al. (2013) Distinct Clinical Characteristics of C9orf72 Expansion Carriers Compared With GRN, MAPT, and Nonmutation Carriers in a Flanders-Belgian FTLD Cohort. *JAMA Neurol*, 10.1001/2013.jamaneurol.181.
6. Cruts M, et al. (2006) Null mutations in progranulin cause ubiquitin-positive frontotemporal dementia linked to chromosome 17q21. *Nature* 442(7105):920–924.
7. Prengel I (2000) Entwicklung und immunmorphologische Charakterisierung monoklonaler Antikörper gegen Proteine des Zebrabärblings (*Danio rerio*). PhD thesis (Ludwig-Maximilians University, Munich).
8. Weinstein BM, Stemple DL, Driever W, Fishman MC (1995) Gridlock, a localized heritable vascular patterning defect in the zebrafish. *Nat Med* 1(11):1143–1147.
9. Reynolds ES (1963) The use of lead citrate at high pH as an electron-opaque stain in electron microscopy. *J Cell Biol* 17:208–212.
10. Link V, Shevchenko A, Heisenberg CP (2006) Proteomics of early zebrafish embryos. *BMC Dev Biol* 6:1.
11. Wiśniewski JR, Zougman A, Nagaraj N, Mann M (2009) Universal sample preparation method for proteome analysis. *Nat Methods* 6(5):359–362.
12. Boersema PJ, Raijmakers R, Lemeer S, Mohammed S, Heck AJ (2009) Multiplex peptide stable isotope dimethyl labeling for quantitative proteomics. *Nat Protoc* 4(4):484–494.
13. Wiśniewski JR, Zougman A, Mann M (2009) Combination of FASP and StageTip-based fractionation allows in-depth analysis of the hippocampal membrane proteome. *J Proteome Res* 8(12):5674–5678.
14. Cox J, Mann M (2008) MaxQuant enables high peptide identification rates, individualized p.p.b.-range mass accuracies and proteome-wide protein quantification. *Nat Biotechnol* 26(12):1367–1372.
15. Cox J, et al. (2011) Andromeda: A peptide search engine integrated into the MaxQuant environment. *J Proteome Res* 10(4):1794–1805.
16. Hogl S, Kuhn PH, Colombo A, Lichtenthaler SF (2011) Determination of the proteolytic cleavage sites of the amyloid precursor-like protein 2 by the proteases ADAM10, BACE1 and γ-secretase. *PLoS ONE* 6(6):e21337.

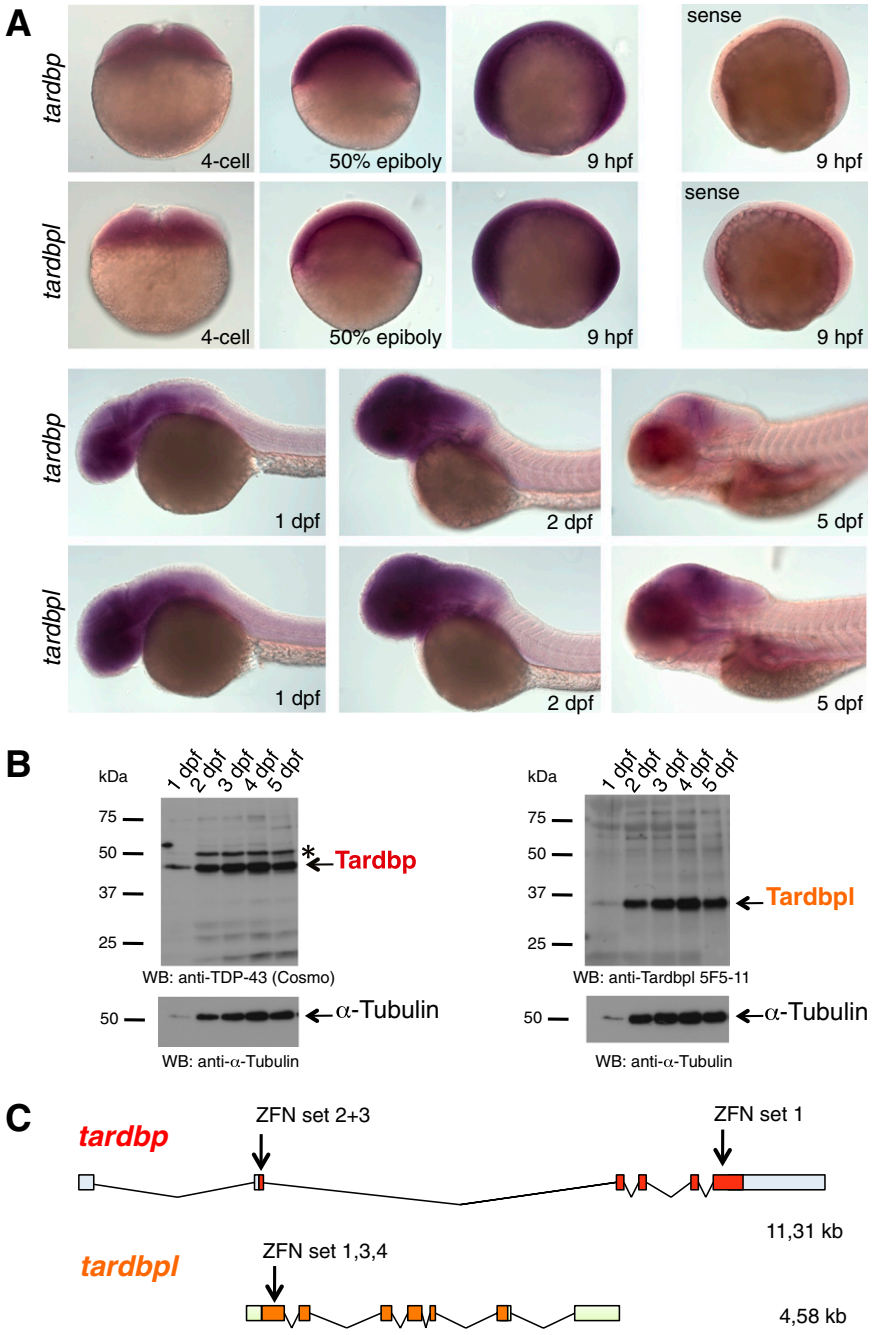

Fig. S1. *Tardbp* and *Tardbpl* are expressed throughout development and overview of zinc finger binding sites of the ZFN. (*A*) In situ hybridization with antisense probes specific for *tardbp* and *tardbpl* during early developmental stages of 4 cell to 5-dpf-old wild-type embryos. Labeling of 9-hpf-old embryos with a sense probe serves as a negative control (magnification: 10×). (*B*, *Left*) Western blot analysis with the Tardbp-specific antibody anti–TDP-43 (Cosmo) reveals expression of Tardbp protein 1 dpf through 5 dpf. The asterisk marks an unspecific band. (*Right*) Western blot analysis with a Tardbpl-specific antibody (anti-Tardbpl 5F5-11) shows that Tardbpl is expressed 1 dpf through 5 dpf. Analysis with an anti–α-Tubulin specific antibody of the respective blots serves as a loading control. (*C*) Schematic representation of the genomic organization of *tardbp* (light blue boxes represent 5′ and 3′ UTR; red boxes represent coding exons) and *tardbpl* (light green boxes represent 5′ and 3′ UTR; orange boxes represent coding exons) locus. Arrows indicate genomic localization of the target sequence of respective ZFN sets.

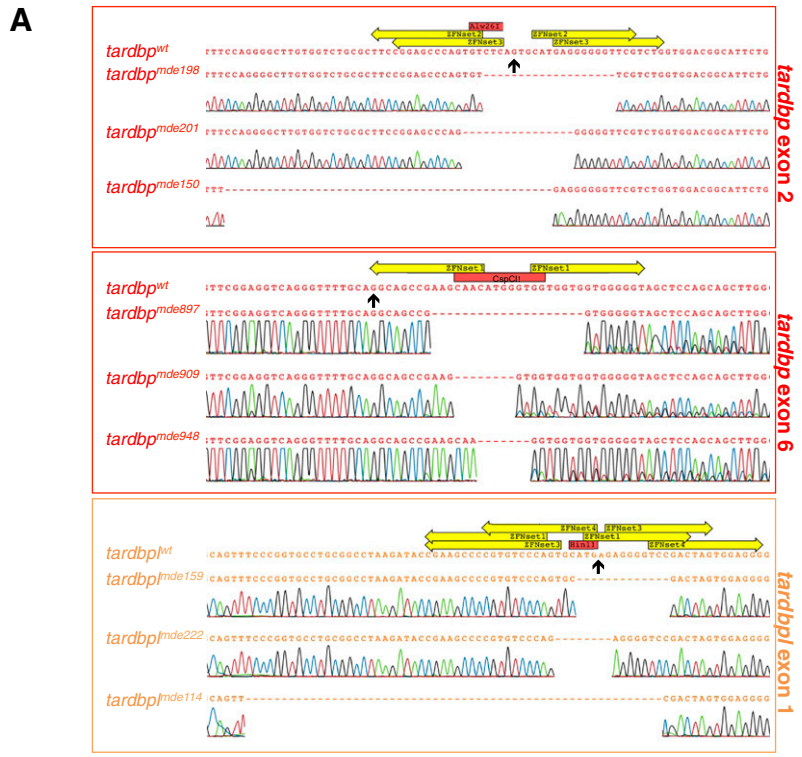

Fig. S2. Location of ZFN binding sites and representation of induced mutations generated by ZFN. (*A*) Three independent mutant lines each were established for ZFN sets targeting *tardbp* exon 2, *tardbp* exon 6, and *tardbpl* exon 1. Sequences of alleles around mutation site are shown with respective allele designation beneath the wild-type sequence. The position of the ZFN sets (yellow), as well as the restriction enzyme recognition site (red) used for identification of the mutation is indicated above the wild-type nucleotide sequence. The arrow underneath the respective wild-type sequences indicates the restriction enzyme cleavage site. (*B*) Sequence alignment of wild-type and mutant Tardbp and Tardbpl alleles with respective allele designation (allele number specifies the last nucleotide of the newly introduced stop codon). Amino acids in italics represent newly introduced amino acids upon frame-shift. Asterisks represent the stop codons.

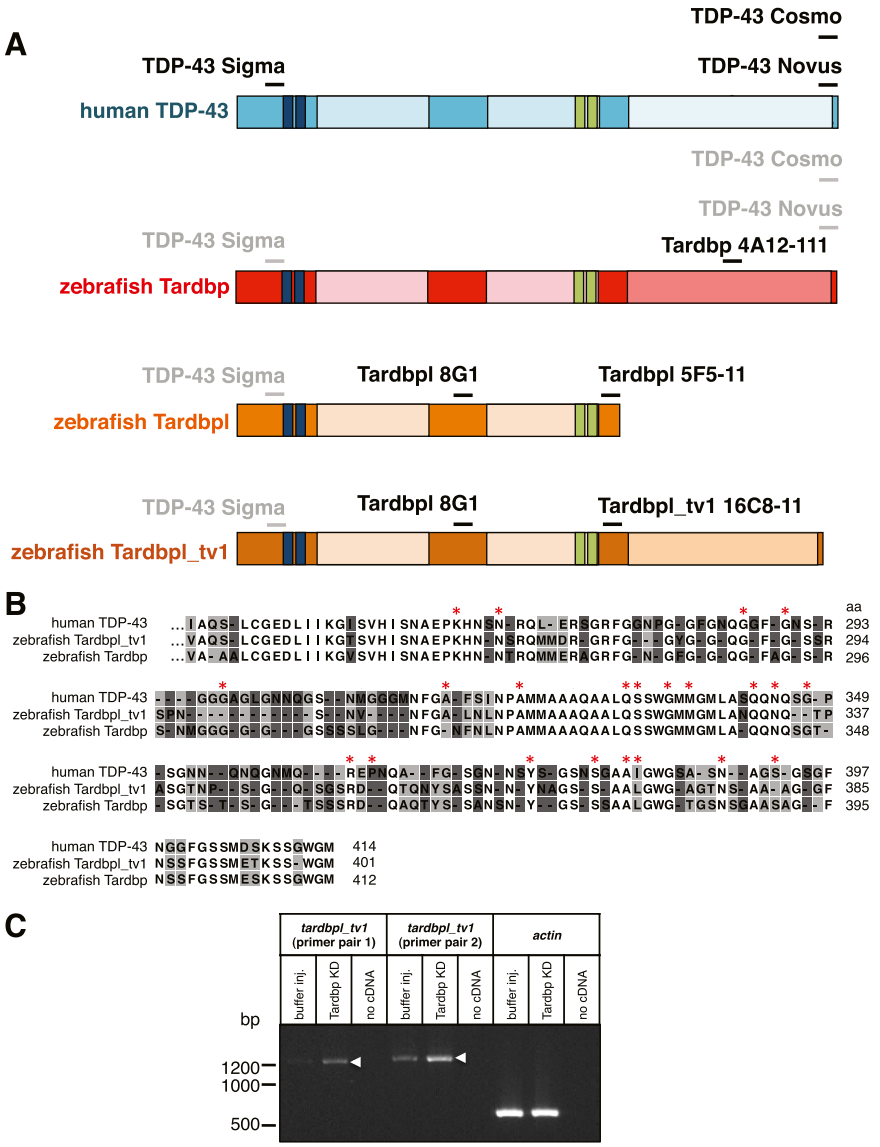

Fig. S3. Schematic representation of antibody binding sites, alignment of C termini of human TDP-43, Tarbpl_tv1, and Tardbp, and up-regulation of *tardbpl_tv1* mRNA upon loss of Tardbp. (*A*) Epitopes of respective antibodies (written in black) are indicated as a black line above the schematically represented proteins (protein domains as in Fig. 1). Lines and antibody names in gray indicate cross-reactivity of antibodies raised against human TDP-43 protein with the corresponding epitopes of zebrafish homologs. (*B*) Amino acid alignment of exon 5 of Tardbpl_tv1 with the corresponding sequence of zebrafish Tardbp and human TDP-43 (identical amino acids are not highlighted, identical amino acids in two of the three amino acids are highlighted in light gray and nonidentical amino acids are highlighted in dark gray). Amino acids mutated in ALS/FTLD patients are marked with a red asterisk. (*C*) Semiquantitative RT-PCR with primers specific for *tardbpl_tv1* (*tardbpl_tv1* primer pair 1 and 2) and *actin* as a loading control. Each primer pair is used on cDNA generated from buffer injected control embryos, Tardbp knockdown embryos, or a negative control with no cDNA added, respectively. Arrowheads indicate the up-regulation of *tardbpl_tv1* transcript upon Tardbp KD compared with buffer injected control embryos.

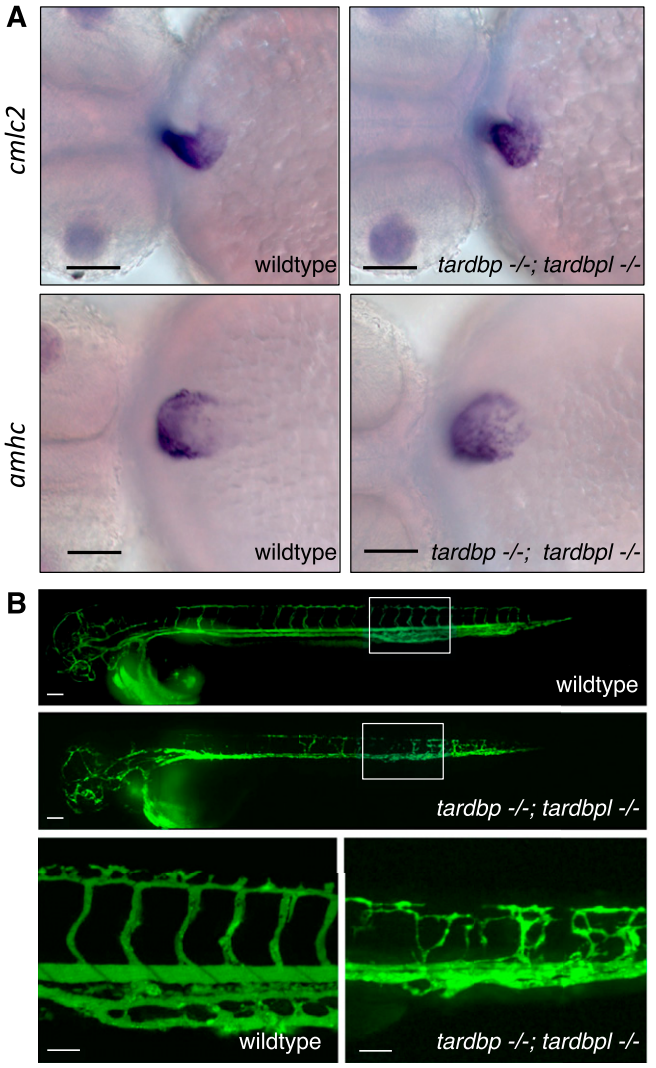

Fig. S4. In situ hybridization of cardiac markers and microangiography in *tardbp*$^{-/-}$;*tardbpl*$^{-/-}$ mutants. (*A*) *cmlc2* primarily stains the ventricle whereas *amhc* primarily stains the atrial myocardium. These markers do not reveal any obvious differences in wild-type and *tardbp*$^{-/-}$;*tardbpl*$^{-/-}$ embryos. (Scale bars, 100 μm.) Ventral view, anterior to the left, 2 dpf. (*B*) Green fluorescently labeled beads were microinjected into the lumen of the blood vessels (microangiography) to visualize the lumen of the vasculature. (*Top*) A wild-type embryo; (*Middle*) a *tardbp*$^{-/-}$;*tardbpl*$^{-/-}$ mutant. (Scale bar, 100 μm.) (*Bottom*) Higher magnifications of the area in the white box of the upper panels. (Scale bars, 50 μm.) Lateral view, anterior to the left, 2 dpf.

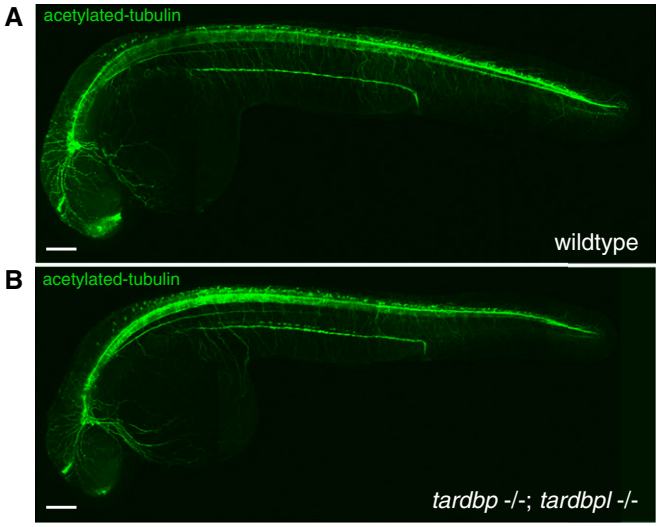

Fig. S5. General neuronal outgrowth is not affected in *tardbp*$^{-/-}$;*tardbpl*$^{-/-}$ mutants. (*A*) Acetylated Tubulin staining demonstrates normal overall axonal patterning in wild-type and (*B*) *tardbp*$^{-/-}$;*tardbpl*$^{-/-}$ embryos at 2 dpf. Lateral view, Anterior to the left. Images are composites of four images, each aligned by Axiovison (Zeiss) software. (Scale bars, 100 μm.)

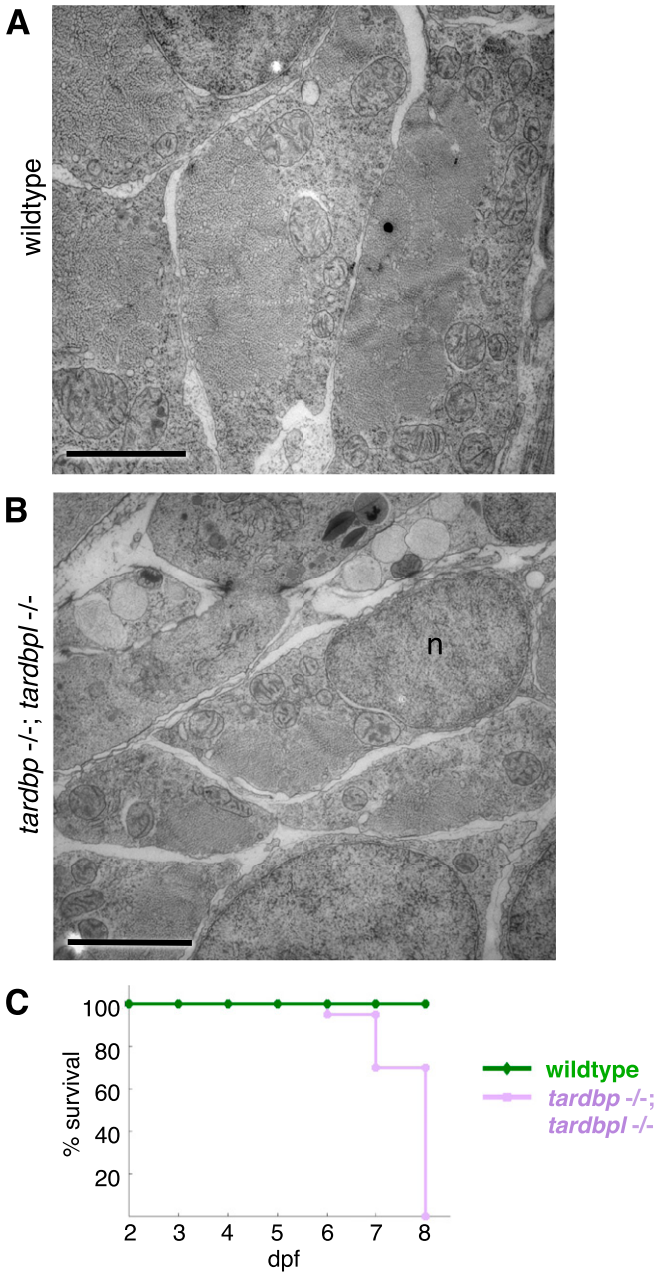

Fig. S6. Ultrastructural morphology of myocytes in *tardbp*$^{-/-}$;*tardbpl*$^{-/-}$ mutants analyzed by EM and early lethality. (*A*) Skeletal muscles of a wild-type embryo display an ordered array of myofibrils surrounded by a highly ordered network of sarcoplasmic reticulum (here shown in cross-sections). Each of the myofibrils is clearly separated by a string of sarcoplasmic reticulum. (*B*) Skeletal muscle of a *tardbp*$^{-/-}$;*tardbpl*$^{-/-}$ mutant embryo shows a highly disorganized pattern of thinner myofibrils with disorganized network of sarcoplasmic reticulum at 2 dpf.. (Scale bars, 2 μm.) *n* = nucleus. (*C*) Kaplan–Meier plot of wild-type (green) and *tardbp*$^{-/-}$;*tardbpl*$^{-/-}$ mutant (purple) embryos. All *tardbp*$^{-/-}$;*tardbpl*$^{-/-}$ mutant embryos analyzed were dead by 8 dpf (*n* = 20), whereas all wild-type embryos were alive (*n* = 20).

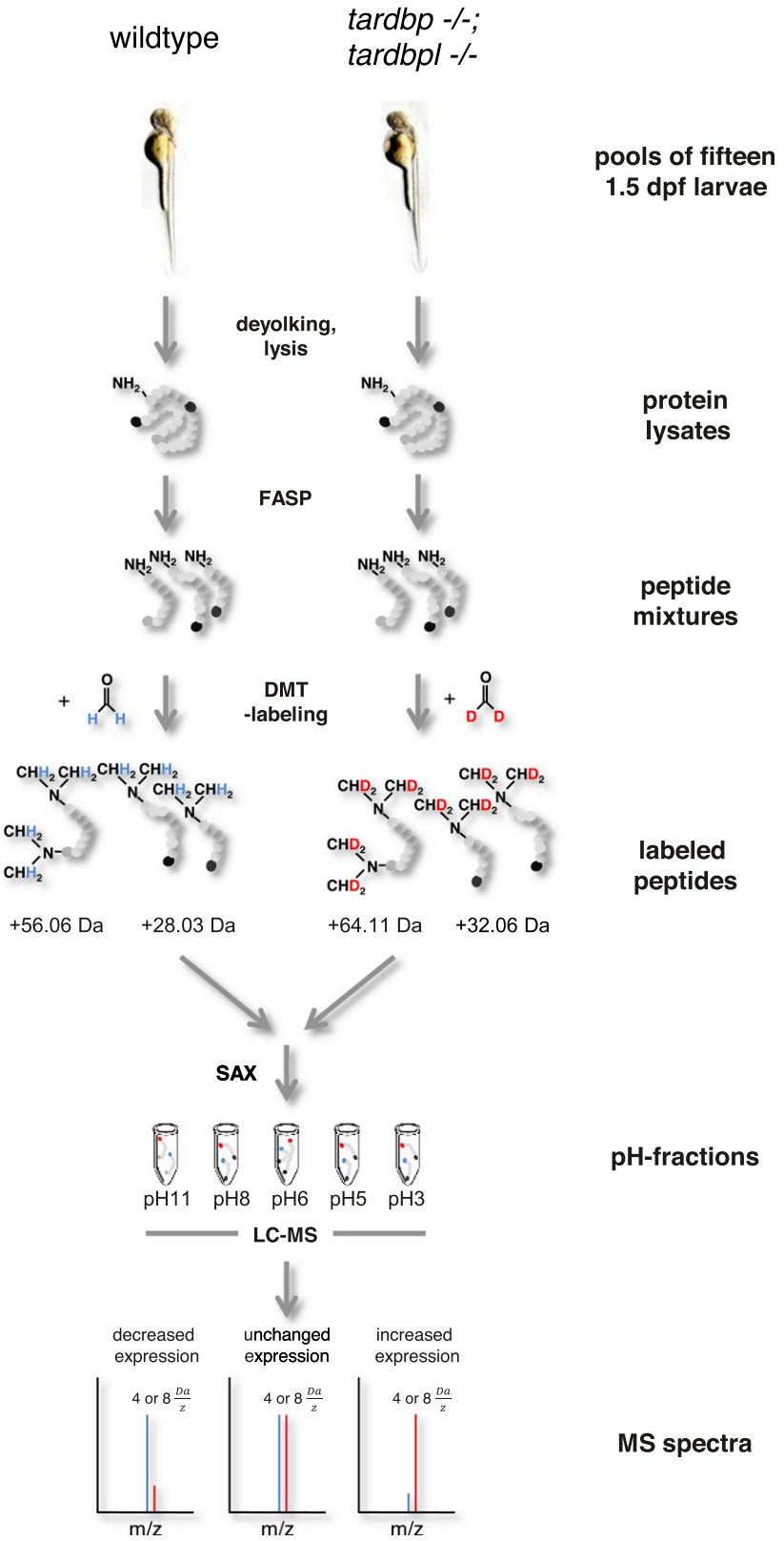

Fig. S7. Schematic view of the quantitative proteomic analysis. Pools of 16 1.5-dpf embryos were deyolked and lysed consecutively. Protein lysates were tryptically digested using the filter-assisted sample preparation technique (FASP). Tryptic peptides ending either on arginine (depicted in black) or a lysine (depicted in dark gray) were labeled using differential stable isotope dimethyl labeling (DMT-labeling). Peptides gained from wild-type embryos were labeled "light" using undeuterated formaldehyde, whereas peptides gained from *tardbp*$^{-/-}$;*tardbpl*$^{-/-}$ mutant embryos were labeled "heavy" using deuterated formaldehyde. Dimethylation occurs at free amine-groups resulting in the addition of four methyl-groups to lysine-containing tryptic peptides whereas only two methyl-groups are added to arginine-containing tryptic peptides; this results in a shift of +56.06 Da or +28.03 Da, respectively, for the light-labeled

Legend continued on following page

peptides. Heavy-labeled peptides are shifted by further +8 Da or +4 Da, respectively, because of the two deuterium atoms contained in every methyl-group. After labeling, peptides from both experimental groups were combined and fractionated using stage-tip-based anion-exchange chromatography (SAX). Mass spectrometry was done for every of the five pH-fractions in two technical replicates. Abundance levels of peptides can be calculated from the intensity ratio between the isotope clusters resulting from the light and heavy peptides.

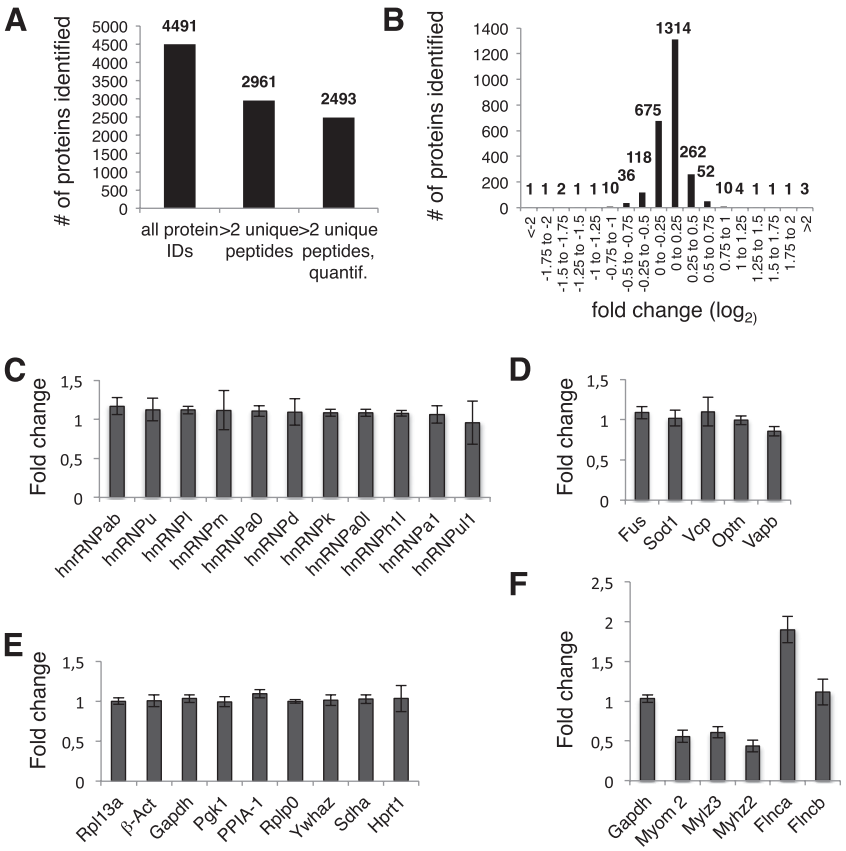

Fig. S8. Proteins analyzed in *tardbp*$^{-/-}$;*tardbpl*$^{-/-}$ mutants. (*A*) Overall, 4,491 proteins could be identified with a false discovery rate below 1%. Of those proteins, 2,961 were identified with at least two different unique peptides and 2,493 of them were quantifiable, meaning that an H/L ratio was determinable for the respective protein in at least two of the three biological replicates. (*B*) Binned distribution of protein expression ratios. Expression ratios were $\log_2$-transformed and further the number of proteins per predefined bin was counted (bin size 0.25). Number of proteins per bin is given. The distribution shows that most of the quantifiable proteins show unchanged levels in the *tardbp*$^{-/-}$;*tardbpl*$^{-/-}$ fish. Fold-changes between *tardbp*$^{-/-}$;*tardbpl*$^{-/-}$ and wild-type are given for (*C*) detected heterogeneous ribonucleoproteins and (*D*) proteins implicated in ALS and FTLD pathology. (*E*) Ratios of the levels of typical reference genes are not altered. (*F*) In contrast to the housekeeping protein Gapdh, muscle-specific proteins Myomesin2 (Myom2), Fast skeletal muscle myosin light polypeptide 3 (Mylz3), and fast muscle myosin heavy polypeptide 2 (Myhz2) are down-regulated. Filamin Ca (Flnca) is up-regulated and Filamin Cb (Flncb) expression is not changed.

Table S1. Summary of rescue experiments of circulation defects in *tardbp*$^{-/-}$;*tardbpl*$^{-/-}$ mutants

RNA injected	% of expected phenotype	No. embryos control/injected	No. clutches	*P* value
TDP-43	41.9	457/488	6	0.0005
tardbpl_tv1	45.1	253/182	2	0.0230
tardbpl	99.7	206/267	3	0.9845
TDP-43^{G348C}	61.3	286/290	3	0.0469
FUS	103.3	293/248	5	0.7371

Rescues were performed by injection of mRNAs encoding human TDP-43, zebrafish Tardbpl_tv1, zebrafish Tardbpl, human TDP-43^{G348C}, or human FUS. The phenotype of the 25% of double-homozygous mutants of a *tardbp*$^{-/-}$;*tardbpl*$^{+/-}$ or *tardbp*$^{+/-}$;*tardbpl*$^{-/-}$ mating were set to 100%. All clutches were split and half of the clutch was injected with the respective mRNA, or served as a control, respectively (No. embryos control/injected). No. clutches indicates the number of clutches analyzed. *P* value were determined by Student's *t* test.

Table S2. Quantitative mass spectrometry analysis of *tardbp*$^{-/-}$;*tardbpl*$^{-/-}$ mutants (up-regulated proteins)

Protein names	Gene names	Accession	Peptides	Unique peptides	PEP	Ratio Ex. 1	Ratio Ex. 2	Ratio Ex. 3	Mean Ratio	SEM	*P* value
Filamin Ca	*flnca*	IPI00489109	20	8	1.01E-142	2.02	1.82	1.86	1.90	0.06	0.0045
Transcription factor Stat3	*stat3*	IPI00484946	4	4	1.66E-67	1.55	1.65	NQ	1.60	0.05	0.0472
Nicastrin	*ncstn*	IPI00487984	4	4	5.12E-09	NQ	1.50	1.51	1.50	0.01	0.0000
COX17 cytochrome *c* oxidase assembly homolog (*Saccharomyces cerevisiae*)	*cox17*	IPI00492717	2	2	6.38E-06	1.44	1.51	NQ	1.47	003	0.0396
ATPase, aminophospholipid transporter, class I, type 8B, member 1	*atp8B1*	IPI00993144	4	4	5.22E-12	1.39	1.55	1.41	1.46	0.05	0.0123
PD2-like protein	*paf1l*	IPI00611430	6	6	7.38E-126	1.44	1.45	1.22	1.40	0.07	0.0433
Neurocalcin-delta A	*ncalda*	IPI00503951	4	2	7.64E-11	1.44	1.23	1.47	1.38	0.07	0.0420
Cathepsin B	*ctsb*	IPI00485996	3	3	1.65E-81	1.34	1.29	1.49	1.37	0.06	0.0263
Polypyrimidine tract binding protein 1b	*ptbp1b*	IPI00613822	6	3	1.68E-140	NQ	1.36	1.39	1.37	0.01	0.0029
Zgc:55819 (endoplasmic reticulum lectin 1)	*erlec1*	IPI00506803	2	2	6.03E-09	1.36	1.30	NQ	1.33	0.03	0.0500
Zeta2-cop	*copz2*	IPI00492912	3	3	3.69E-08	1.23	1.29	1.45	1.32	0.06	0.0441
Transducin (β)-like 2	*tbl2*	IPI00962763	4	4	1.37E-12	1.28	1.27	1.41	1.32	0.04	0.0211
Zgc:101838 (tetratricopeptide repeat domain 1)	*ttc1*	IPI00996124	5	5	5.07E-08	1.31	1.32	NQ	1.31	0.01	0.0001

Hits from the quantitative proteomic analysis of the *tardbp*$^{-/-}$;*tardbpl*$^{-/-}$ mutants grouped into up-regulated proteins. Inclusion criteria for a hit were: at least 30% increased or decreased abundance, successful quantification in at least two biological replicates, at least two unique peptides identified and a *P* value < 0.05 (Student *t* test). Protein name, gene name, IPI accession number, the number of identified unique peptides, the posterior error probability (PEP), the ratio of the protein abundance in the three different biological replicates (Ratio Ex. 1–3), the resulting mean ratio, the SEM ratio (SEM), and the calculated *P* value are given. Protein ratios, which could not be determined in a respective biological replicate, are marked as not quantifiable (NQ). The low amounts of the hemoglobin proteins in the mutants are presumably a preparation artifact, because blood cells accumulate on the yolk in the mutants specifically and most likely are manually removed during the deyolking step for sample preparation.

Table S3. Quantitative mass spectrometry analysis of *tardbp*$^{-/-}$;*tardbpl*$^{-/-}$ mutants (down-regulated proteins)

Protein names	Gene names	Accession	Peptides	Unique peptides	PEP	Ratio Ex. 1	Ratio Ex. 2	Ratio Ex. 3	Mean Ratio	SEM	*P* value
Parvalbumin 1	*pvalb1*	IPI00494456	6	3	1.88E-127	0.62	0.76	0.71	0.70	0.04	0.0108
Myomesin 1a	*myom1a*	IPI00493389	26	25	8.37E-143	0.68	0.78	0.61	0.69	0.05	0.0201
Dystrophin	*dmd*	IPI00510896	10	9	3.85E-28	0.80	0.57	0.58	0.69	0.08	0.0355
Apolipoprotein A1	*apoa1*	IPI00495830	21	20	8.99E-228	0.83	0.59	0.64	0.69	0.07	0.0409
Cytosolic 5-nucleotidase 3	*nt5c3*	IPI01024291	4	4	6.50E-29	NQ	0.68	0.68	0.68	0.00	0.0003
Ryanodine receptor 1b	*ryr1b*	IPI00771673	22	21	1.42E-124	0.67	0.78	0.53	0.66	0.07	0.0350
Slow myosin heavy chain 1	*smyhc1*	IPI00934366	116	6	0	068	0.72	0.54	0.65	0.05	0.0182
Atrial myosin light chain	*zgc:66286*	IPI00509545	10	7	5.58E-132	0.60	0.77	0.56	0.64	0.06	0.0248
Parvalbumin 4	*pvalb4*	IPI00507878	5	3	1.39E-15	0.75	0.69	0.49	0.64	0.08	0.0373
Fast muscle troponin T isoform TnnT3b	*tnnt3b*	IPI00817433	10	8	4.42E-180	0.76	0.57	0.58	0.64	0.06	0.0207
Type IV antifreeze protein	*zgc:161979*	IPI00637112	6	5	6.81E-19	0.78	0.50	0.62	0.63	0.08	0.0366
Cardiac muscle myosin heavy chain 6 alpha	*myh6*	IPI00490216	45	2	0	0.57	0.79	0.47	0.61	0.09	0.0452
Fast skeletal muscle myosin light polypeptide 3	*mylz3*	IPI00488248	13	9	3.77E-135	0.58	0.75	0.51	0.61	0.07	0.0261
Myosin binding protein H	*LOC570313*	IPI00502301	14	14	1.67E-183	0.60	0.68	0.53	0.60	0.04	0.0083
Myosin binding protein C, fast type b	*mybpc2b*	IPI00484548	24	24	5.00E-230	0.61	0.68	0.51	0.60	0.05	0.0121
Desmoplakin	*dsp*	IPI00802893	8	8	7.02E-68	0.61	0.48	0.70	0.60	0.06	0.0187
Myomesin 3	*myom3*	IPI00900800	24	21	7.08E-151	0.56	0.67	0.55	0.60	0.04	0.0054
Calsequestrin	*casq2*	IPI00492700	6	6	1.76E-40	0.62	0.64	0.50	0.59	0.04	0.0080
Myosin light chain, phosphorylatable, fast skeletal muscle	*mylpflb*	IPI00496651	15	6	0	0.53	0.76	0.45	0.58	0.09	0.0395
Parvalbumin 3	*pvalb3*	IPI00492274	6	2	7.35E-18	0.54	NQ	0.60	0.57	0.03	0.0261
Novel protein similar to H.sapiens TTN, titin (TTN)	*CH211-198B21.1–001*	IPI00851394	66	4	0	0.58	0.53	0.59	0.56	0.02	0.0006
Myomesin 2	*myom 2*	IPI00960438	3	3	1.65E-18	0.63	0.57	0.38	0.56	0.07	0.0204
Myosin, heavy chain 7B, cardiac muscle, beta	*myh7b*	IPI00501288	22	2	1.22E-233	0.56	0.57	0.51	0.55	0.02	0.0005
Myosin, heavy polypeptide 2, fast muscle specific	*myhz2*	IPI00933204	151	6	0	0.48	0.54	0.29	0.44	0.08	0.0150
Embryonic globin beta 3	*hbbe3*	IPI00496135	9	9	1.88E-171	0.35	0.26	0.31	0.31	0.02	0.0004
Embryonic globin alpha 3	*hbae3*	IPI00492692	4	3	3.44E-36	0.31	0.23	0.37	0.30	0.04	0.0023
Embryonic globin beta 1	*hbbe1*	IPI00502256	9	9	1.90E-101	0.30	0.20	0.34	0.28	0.04	0.0024
TAR DNA binding protein, like	*tardbpl*	IPI00504192	7	5	6.23E-78	0.20	0.12	0.11	0.16	0.03	0.0007

Hits from the quantitative proteomic analysis of the *tardbp*$^{-/-}$;*tardbpl*$^{-/-}$ mutants grouped into down-regulated proteins. Inclusion criteria for a hit were: at least 30% increased or decreased abundance, successful quantification in at least two biological replicates, at least two unique peptides identified and a *P* value < 0.05 (Student *t* test). Protein name, gene name, IPI accession number, the number of identified unique peptides, the posterior error probability (PEP), the ratio of the protein abundance in the three different biological replicates (Ratio Ex. 1–3), the resulting mean ratio, the SEM ratio (SEM), and the calculated *P* value are given. Protein ratios, which could not be determined in a respective biological replicate, are marked as not quantifiable (NQ). The low amounts of the hemoglobin proteins in the mutants are presumably a preparation artifact, because blood cells accumulate on the yolk in the mutants specifically and most likely are manually removed during the deyolking step for sample preparation.

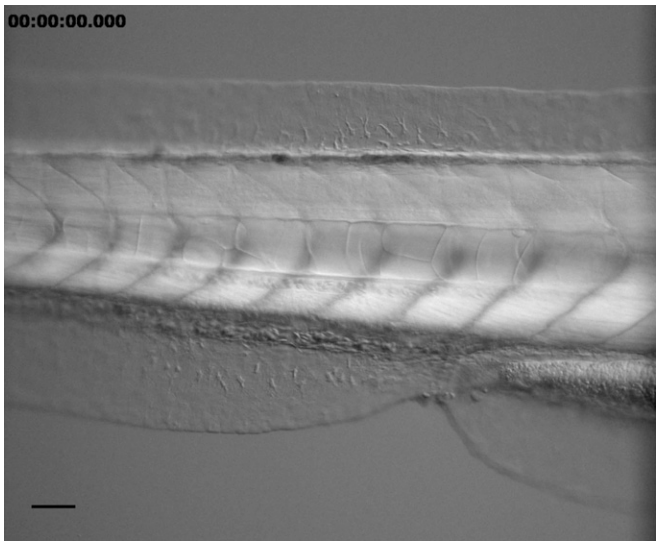

Movie S1. The movie shows a wild-type embryo with normal circulation of erythrocytes (2 dpf, lateral view of the trunk, anterior to the right). (Scale bar: 50 μm.)

Movie S1

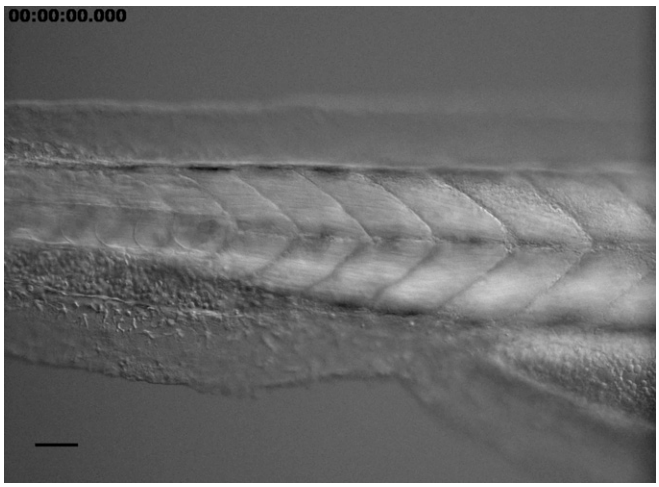

Movie S2. The movie shows the lack of circulating erythrocytes in *tardbp*$^{-/-}$;*tardbpl*$^{-/-}$ embryos (2 dpf, lateral view of the trunk, anterior to the right). (Scale bar: 50 μm.)

Movie S2

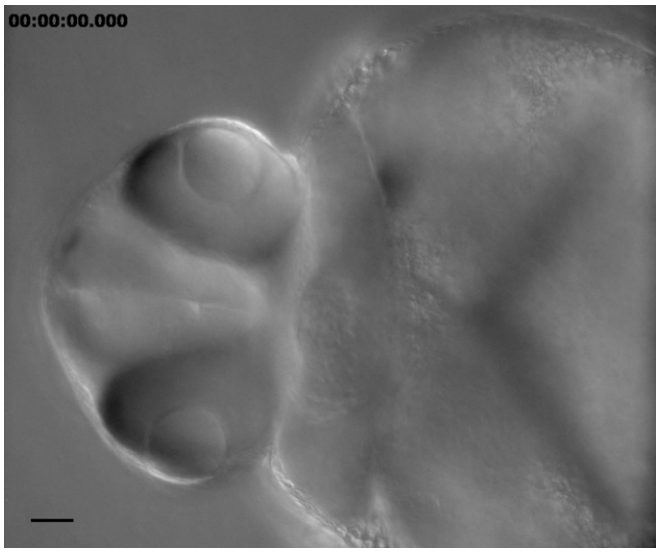

Movie S3. The movie shows the beating heart of a wild-type embryo (2 dpf, ventral view on the heart, anterior to the left). (Scale bar: 50 μm.)

Movie S3

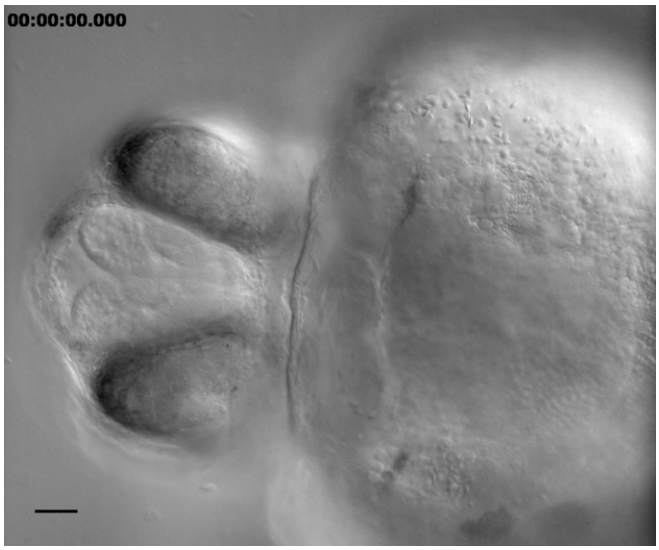

Movie S4. The movie shows a beating heart in *tardbp*$^{-/-}$;*tardbpl*$^{-/-}$ embryos (2 dpf, ventral view on the heart, anterior to the left). (Scale bar: 50 μm.)

Movie S4

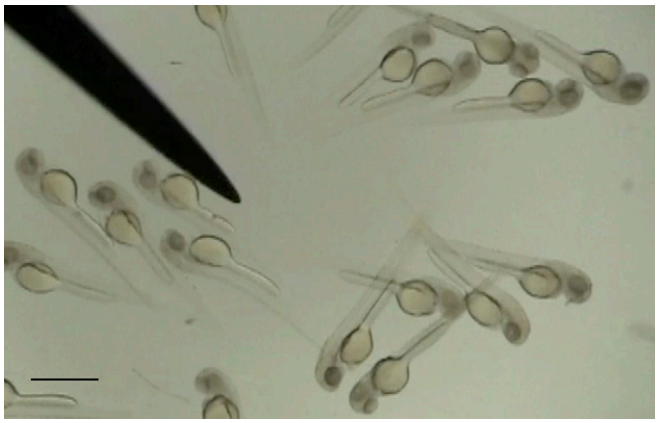

Movie S5. *tardbp*$^{-/-}$;*tardbpl*$^{-/-}$ embryos have a movement phenotype. Video recordings of the escape response of wild-type and *tardbp*$^{-/-}$;*tardbpl*$^{-/-}$ embryos at 2 dpf upon touch stimulus. (Scale bar: 1 mm.)

Movie S5